Uniqueness, stability analysis and approximate solution of a fractional order COVID-19 Model

Muhammad Umer Saleem[a], Khadija Jamil[b], Muhammad Farhan Tabassum[c]

[a]Department of Mathematics, University of Education, Lahore, Pakistan.

[b]Department of Mathematics, Khawaja Fareed University of Engineering and Information Technology, Rahim Yar Khan, Pakistan.

[c]Department of Mathematics, University of Management and Technology, Lahore, Pakistan.

Corresponding author Email:umerlinks@ue.edu.pk

Abstract:

In this paper, we investigate a fractional model for the COVID-19 epidemic that contains an antiretroviral treatment compartment. We implement novel methods to acquire effective results. We discuss equilibrium point, reproductive number, and sensitivity analysis. We utilize the Sumudu transform technique to obtain approximate solutions for the model, and we explore chaos control to assess stability around equilibrium points. We demonstrate the numerical simulations to prove the accuracy of the proposed techniques. The graphs illustrate how varying fractional orders impact the dynamics of each epidemiological group, revealing the memory and time-dependent effects on disease spread and control strategies.

Keywords: Sumudu transform; Uniqueness; Sensitivity Analysis; Numerical Scheme

1. Introduction

The number of infections rises rapidly as long as COVID-19 outbreaks persist. This is due to several features that make COVID-19 infections more complicated and provide challenges for managing the disease [1-3]. Oxygen therapy is also used in persons who feel suffocating. Immunity booster is also required for the infected, suspected, and even healthy person because if a person's immune system is strong then he/she can fight with any disease including COVID-19 [4]. There are many preventive measures for COVID-19. Maintaining 1 meter or 3 feet distance from another person is the most important and useful preventive measure and it is known as social distancing. Other preventive measures include wearing a mask properly, using sanitizer, and washing hands for at least 20 seconds [5]. Scientists who were already working on the coronavirus took part in this workshop. They presented and discussed different mathematical

models which develop evidence. After four months the workshop gave chance to participants that they openly discuss issues they face in developing mathematical modeling of corona virus. Different mathematical models were presented but the main model was epidemiological model [6].

In [7–12], the notion of the fractional derivative is elucidated. Atangana et al. proposed [13] a numerical technique for investigating a nonlinear fractional differential equation. In [14] to gain a better comprehension of solutions to singular fractional differential equations. In [15] discusses the uniqueness and the existence of positive solutions to the integral boundary value problem that encompasses the fractional integro-differential equation. The proposed viral outbreak [16–18] accurately captures the temporal trajectory of the conceptual model of COVID-19 illness. The evaluation of the novel coronavirus risk of transmission has been discussed by Tang et al. [19]. The predominant feature observed within these models pertains to their global (non-local) characteristics, which encompass fractional applications and are additionally addressed in [20–23]. Many schemes have been used according to the references given above but we have used this scheme because this scheme is more useful and its effects have proved to be more effective than other schemes [24-26]. The significance of immigration and closely contacted individuals in managing COVID-19 is emphasized by the study [27]. It demonstrates that controlling incubation delays and implementing efficient control mechanisms are essential for the effectiveness of containment. To more accurately forecast and control the spread of disease, the study [28] highlights the significance of including nonlinear dynamics in epidemic models.

The study of a fractional-order COVID-19 model innovative mathematical techniques, such as the Atangana-Baleanu and Caputo derivatives, to capture the dynamics of the pandemic more accurately. This approach not only proves the existence and uniqueness of the solutions to the posed problems but also takes into account memory effects which represent the modelling of the infection spread and the control measures such as the lockdown. The study thus brings addition to the theoretical knowledge on epidemic modeling and contributes to the development of efficient applied population health interventions. This research is a valuable resource for comprehending the transmission and control of the pandemic. The fractal fractional operator better captures complex, memory-driven dynamics, reflecting the irregular nature of real-world phenomena like COVID-19 spread. It more accurately models anomalous diffusion and long-range interactions, enhancing predictive power in epidemiological modeling. Fractional models, in contrast to standard models, take memory effects and non-local dynamics into consideration, better simulating the nature of infectious diseases. Employing the Mittag-Leffler kernel in

conjunction with the ABC fractional derivative within COVID-19 modeling facilitates the integration of memory phenomena, thereby enhancing the model's realism by accommodating long-term impacts. The non-singular ABC derivative yields smoother and more stable computational outcomes, effectively circumventing complications associated with infinite singularities. These methodologies provide significant flexibility in calibrating the model to align with empirical data, thereby augmenting the precision of forecasts. Furthermore, they effectively capture anomalous diffusion, which is critical for accurately depicting irregular patterns of infection dissemination. Consequently, this approach results in more precise and adaptable models suited for dynamic scenarios associated with pandemics.

In this paper, we formulated a fractional order COVID-19 model that is based on Atangana-Baleanu fractional derivatives and the Atangana-Toufik scheme. In Section 1, we formulate the introductory segment accompanied by a comprehensive literature review about COVID-19 and fractional calculus. Section 2 contains fundamental definitions that are useful for analyzing and simulating the model. In Section 3, a mathematical model of COVID-19 is presented, discussing the boundedness and positivity of the model. The system of solutions for the model's existence and uniqueness has been confirmed in Section 4 using fixed point theory and an iterative method. In Sect. 5 we discuss chaos control to check stability at equilibrium point. In Sect. 6, the New Numerical scheme is constructed with the Atangana-Toufik method for real data from Saudi Arabia. We detail the numerical simulation of the suggested method using real data and the substitution of the best-fitting parameters in section 7. In section 8, we offer the conclusions and opinions.

2. Preliminaries

Definition 2.1: The Atangana-Baleanu fractional-order derivative in the Liouville-Caputo sense is defined as specified [12].

$$^{ABC}_{w}D^{\omega}_{t}\big(\vartheta(t)\big) = \frac{AB(\omega)}{m-\omega}\int_{w}^{t}\frac{d^m}{de^m}f(e)P_{\omega}\left\{-\omega\frac{(t-e)^{\omega}}{m-\omega}\right\}de, \ \ m-1 < \omega < m. \tag{1}$$

To derive the Laplace transform of Equation (1)

$$L[^{ABC}_{w}D^{\omega}_{t}\vartheta(t)](q) = \frac{AB(\omega)}{1-\omega}\frac{q^{\omega}L[\vartheta(\tau)](q) - q^{\omega-1}\vartheta(0)}{q^{\omega} + \frac{w}{1-w}}. \tag{2}$$

Applying the Sumudu transform (ST) to (1) yields

$$ST[^{ABC}_0D^\omega_t\vartheta(t)](q) = \frac{B(\omega)}{1-\omega}\left\{\omega\Gamma(\omega+1)P_\omega\left(-\frac{1}{1-\omega}e^\omega\right)\right\} \times [ST(\vartheta(t)) - \vartheta(0)]. \qquad (3)$$

Definition 2.2: Given a function $\vartheta(t)$, the Atangana–Baleanu [17,18] fractional integral of order ω is given by

$$^{ABC}_wI^\omega_t(\vartheta(t)) = \frac{1-\omega}{B-\omega}\vartheta(t) + \frac{\vartheta}{B(\vartheta)\Gamma(\vartheta)}\int_w^t \vartheta(e)(t-e)^{\omega-1}de. \qquad (4)$$

3. SEIQR COVID-19 Model

This section provides an analysis of the principal group S(t), which is delineated as the demographic of healthy individuals who are susceptible to disease acquisition. The population that has been exposed or those who are infected yet not exhibiting contagious symptoms is designated as group E(t). The demographic that has been definitively confirmed as infected is symbolized by group I(t). The population under quarantine, which is segregated from the general public even within their domestic environments, is classified as group Q(t). The population that has successfully recovered is defined as group R(t), as illustrated in Fig. 1.
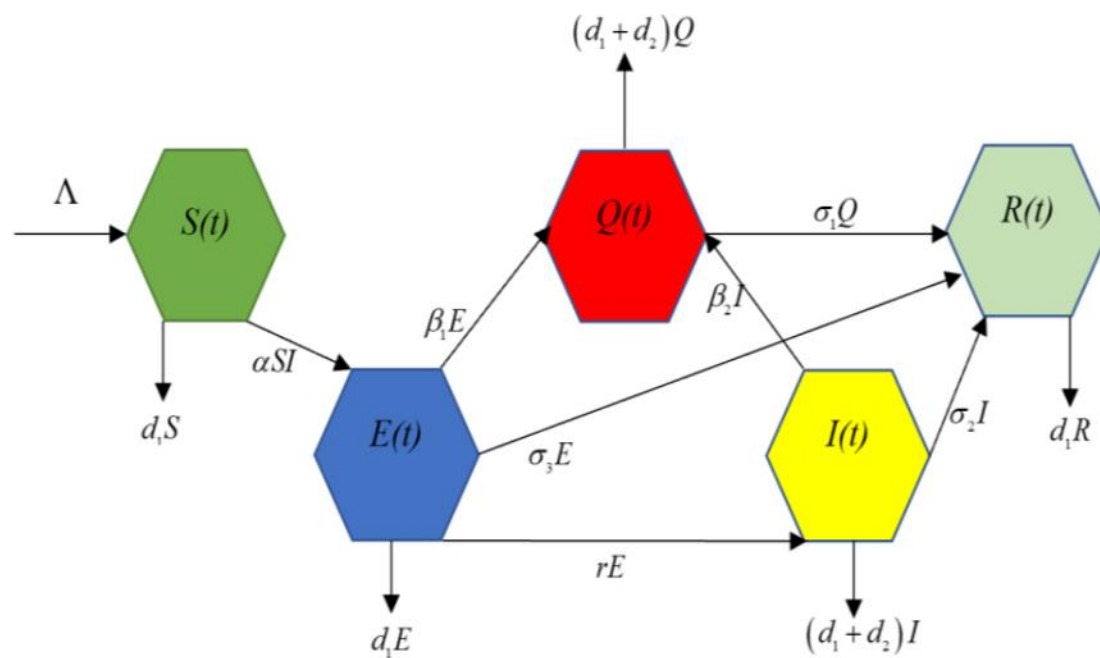
Figure 1: The flowchart of COVID-19 model

The differential equation system in [29] by applying the Atangana-Baleanu fractional derivative of order α and $\alpha \in (0,1]$, into Mittag-Leffler kernel, then the system of equations becomes

$${}^{ABC}_{0}D^{\alpha}_{t}S = \Lambda - \alpha S(t)I(t) - d_1 S(t),$$

$${}^{ABC}_{0}D^{\alpha}_{t}E = \alpha S(t)I(t) - \varepsilon_1 E(t),$$

$${}^{ABC}_{0}D^{\alpha}_{t}I = rE(t) - \varepsilon_2 I(t),$$

$${}^{ABC}_{0}D^{\alpha}_{t}R = \sigma_3 E(t) + \sigma_2 I(t) - d_1 R(t) + \sigma_1 Q(t),$$

$${}^{ABC}_{0}D^{\alpha}_{t}Q = \beta_1 E(t) + \beta_2 I(t) - \varepsilon_3 Q(t). \tag{5}$$

Where $\varepsilon_1 = (r + \beta_1 + \sigma_3 + d_1)$, $\varepsilon_2 = (\beta_2 + \sigma_2 + d_1 + d_2)$ and $\varepsilon_3 = (\sigma_1 + d_1 + d_2)$.

Initial conditions associated with the system of equations (5). We have

$$S(0) \geq 0, \quad E(0) \geq 0, \quad I(0) \geq 0, \quad R(0) \geq 0, \quad Q(0) =\geq 0.$$

3.1 Positivity and boundedness:

In this part, we address the boundedness and positivity of the suggested model.

Theorem 3.1: A unique and bounded solution for the fractional order system exists inR^{+}_{5}.

Proof: The solution of the mathematical model given in $(10) - (14)$ on the interval $(0, \infty)$ can be subsequently, we need to prove the positive invariant in the non-negative region R^{+}_{5} . We get from the system $(10) - (14)$.

$${}^{ABC}_{0}D^{\alpha}_{t}S \ /_{s=0} = \Lambda \geq 0,$$

$${}^{ABC}_{0}D^{\alpha}_{t}E \ /_{E=0} = \alpha S(t)I(t) - \varepsilon_1 \geq 0,$$

$${}^{ABC}_{0}D^{\alpha}_{t}I \ /_{I=0} = rE(t) \geq 0,$$

$${}^{ABC}_{0}D^{\alpha}_{t}R \ /_{R=0} = \sigma_3 E(t) + \sigma_2 I(t) + \sigma_1 Q(t) \geq 0,$$

$$^{ABC}_0D^\alpha_t Q \ /_{Q=0} = \beta_1 E(t) + \beta_2 I(t) \geq 0.$$

Solutions are bounded in the feasible region and are non-negative in R_5^+. So, the domain R_5^+ is a positively invariant set.

Theorem 3.2: Every model structure solution that starts in R_5^+ has a boundary inside the region ω described $\omega = \left\{ \left(S, E, I, R, Q \in R_5^+ : 0 \leq \ ^{ABC}_0D^\alpha_t N \leq \frac{\Lambda}{d_1} \right) \right\}.$

Proof: From equation (10) -(14), we get

$$^{ABC}_0D^\alpha_t N = \ ^{ABC}_0D^\alpha_t S + \ ^{ABC}_0D^\alpha_t E + \ ^{ABC}_0D^\alpha_t I + \ ^{ABC}_0D^\alpha_t R + \ ^{ABC}_0D^\alpha_t Q.$$

After simplifying, we get

$$^{ABC}_0D^\alpha_t N + d_1 N(t) \leq \Lambda.$$

We get,

$$N(t) \leq \left(N(0) - \frac{\Lambda}{d_1} \right) e^{-d_1 t} + \frac{\Lambda}{d_1}.$$

We have, $t \to \infty$, and we get $N(t) \in \left[0, \frac{\Lambda}{d_1} \right]$, which completes the proof.

3.2 Equilibrium Point:

In the study [28] disease-free equilibrium points of a model (10)-(14) are the following.

$$E_\blacksquare = (S^\blacksquare, E^\blacksquare, I^\blacksquare, R^\blacksquare, Q^\blacksquare) = \left(\frac{\Lambda}{d_1}, 0,0,0,0 \right),$$

the endemic points are given as

$E_\boxtimes = \left(S^\boxtimes, E^\boxtimes, I^\boxtimes, R^\boxtimes, Q^\boxtimes \right)$ where

$$S^\boxtimes = \frac{\varepsilon_1 \varepsilon_2}{r\alpha}, \quad E^\boxtimes = \frac{\varepsilon_2 d_1}{r\alpha} \times \left(\frac{\alpha r \Lambda}{d_1 \varepsilon_1 \varepsilon_2} - 1 \right), \quad I^\boxtimes = \frac{d_1}{\alpha} \times \left(\frac{\alpha r \Lambda}{d_1 \varepsilon_1 \varepsilon_2} - 1 \right),$$

$$R^{\boxtimes} = \left(\frac{\sigma_1(\beta_1 \varepsilon_1 + \beta_2 r) + \sigma_2 r + \varepsilon_2 \sigma_3}{\alpha r} \right) \times \left(\frac{\alpha r \Lambda}{d_1 \varepsilon_1 \varepsilon_2} - 1 \right),$$

$$Q^{\boxtimes} = \left(\frac{(\beta_1 \varepsilon_1 + \beta_2 r) d_1}{\alpha r} \right) \times \left(\frac{\alpha r \Lambda}{d_1 \varepsilon_1 \varepsilon_2} - 1 \right),$$

3.3 Reproductive Number:

The reproductive number R_0, is a key metric in epidemiology that indicates how contagious an infectious disease.

$$R_0 = \frac{\alpha r \Lambda}{d_1(r + \beta_1 + \sigma_3 + d_1)(\beta_2 + \sigma_2 + d_1 + d_2)} = \frac{\alpha r \Lambda}{d_1 \varepsilon_1 \varepsilon_2}.$$
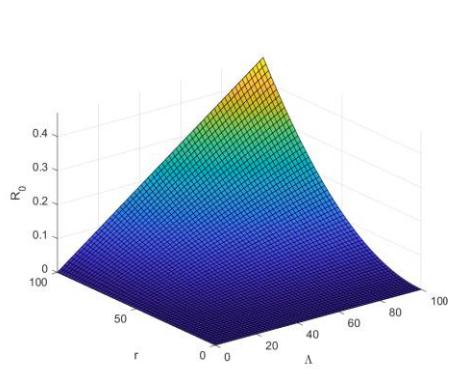
If $R_0 > 0$, it indicates rapid disease spread, requiring immediate and effective intervention. If $R_0 < 0$, it indicates that the disease is under control or declining, but continued monitoring and interventions may be necessary to maintain control. The behavior of different parameters on R_0 is displayed in Figure 2.
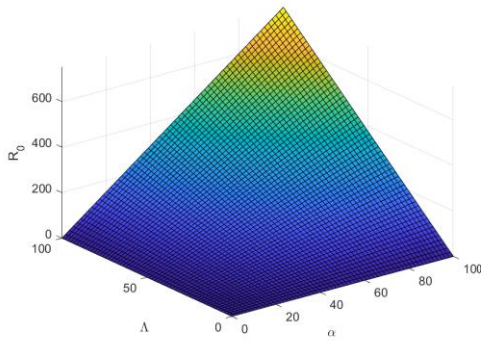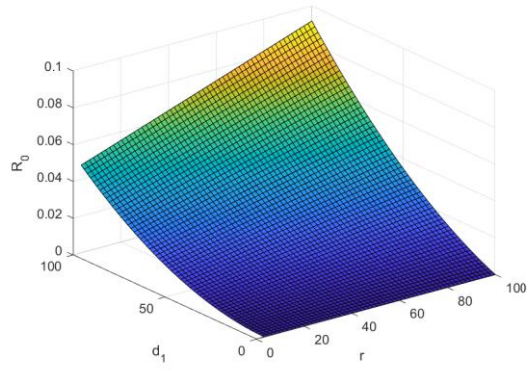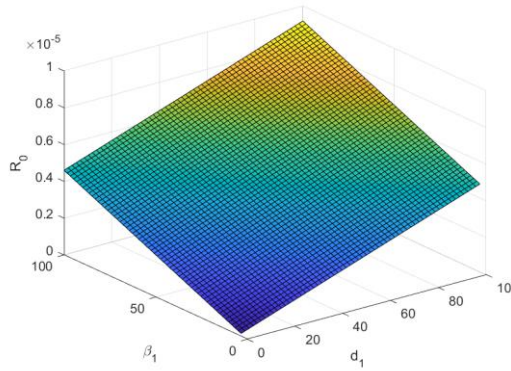

Fig: (a)
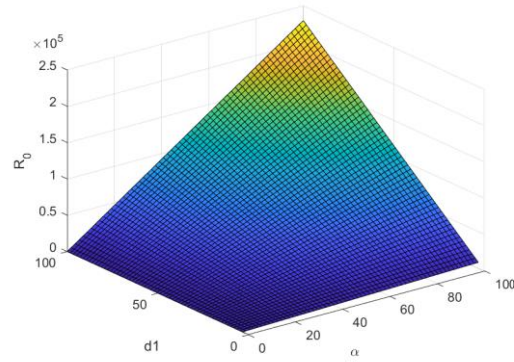
Fig: (b)

Fig: (c)

Fig: (d)

Fig: (e)

Figure 2: Effect of R_0 at different parameters

3.4 Sensitivity Analysis:

Sensitivity analysis in COVID-19 models provides valuable insights into how variations in model parameters influence epidemic dynamics. It aids in understanding the potential impact of different interventions, refining model predictions, and making informed decisions to manage the outbreak effectively. The change in various parameters is shown in Table 1 and Figure 3.

$$\frac{\partial R_0}{\partial \alpha} = \frac{\Lambda r \varepsilon_1 \varepsilon_2}{d_1} \times \frac{\alpha}{R_0} > 0,$$

$$\frac{\partial R_0}{\partial r} = \frac{\Lambda \alpha r \varepsilon_2}{d_1} \times \frac{\Lambda \alpha \varepsilon_1 \varepsilon_2}{d_1} \times \frac{r}{R_0} > 0,$$

$$\frac{\partial R_0}{\partial \Lambda} = \frac{\alpha r \varepsilon_1 \varepsilon_2}{d_1} \times \frac{\Lambda}{R_0} > 0,$$

$$\frac{\partial R_0}{\partial \beta_1} = \frac{\Lambda \alpha r \varepsilon_2}{d_1} \times \frac{\beta_1}{R_0} > 0,$$

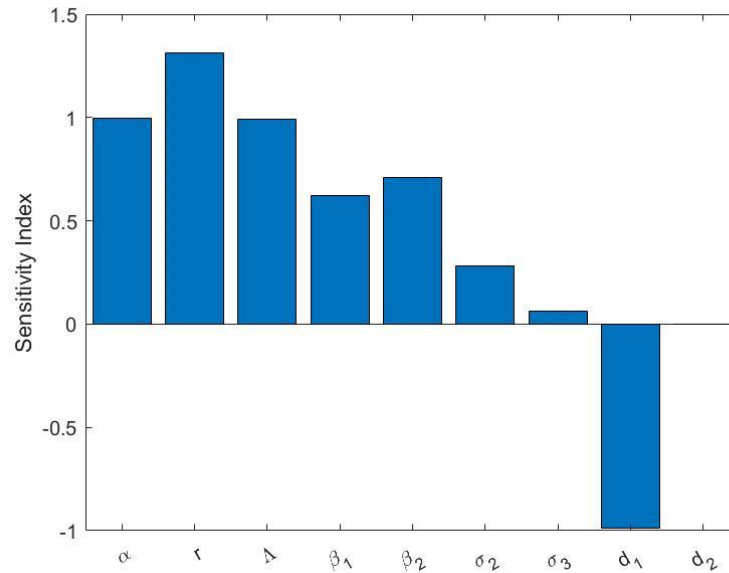$$\frac{\partial R_0}{\partial \beta_2} = \frac{\Lambda \alpha r \varepsilon_1}{d_1} \times \frac{\beta_2}{R_0} > 0, \qquad\qquad \frac{\partial R_0}{\partial \sigma_2} = \frac{\Lambda \alpha r \varepsilon_1}{d_1} \times \frac{\sigma_2}{R_0} > 0,$$

$$\frac{\partial R_0}{\partial \sigma_3} = \frac{\Lambda \alpha r \varepsilon_2}{d_1} \times \frac{\sigma_3}{R_0} > 0, \qquad\qquad \frac{\partial R_0}{\partial d_1} = \frac{\Lambda \alpha r \varepsilon_2}{d_1} + \frac{\Lambda \alpha r \varepsilon_1}{d_1} - \frac{\Lambda \alpha r \varepsilon_1 \varepsilon_2}{d_1^2} \times \frac{d_1}{R_0} < 0,$$

$$\frac{\partial R_0}{\partial d_2} = \frac{\Lambda \alpha r \varepsilon_1}{d_1} \times \frac{d_2}{R_0} > 0,$$

Parameters	Sign	Values
α	+	0.999
r	+	1.312
Λ	+	0.999
β_1	+	0.624
β_2	+	0.711
σ_2	+	0.284
σ_3	+	0.062
d_1	-	-0.990
d_2	+	4.91×10^{-5}

Table 1: Change in parameter values

Figure 3: Sensitivity indices for SEIR Model

4. Mathematical Analysis and Analytical Solution by ABC Operator

By using the Sumudu transform of the system of equations (5), we get

$$\frac{B(\alpha)\alpha\Gamma(\alpha+1)}{1-\alpha} E_\alpha \left(-\frac{1}{1-\alpha}w^\alpha\right) ST\{S(t) - S(0)\} = ST[\Lambda - \alpha S(t)I(t) - d_1 S(t)], \tag{6}$$

$$\frac{B(\alpha)\alpha\Gamma(\alpha+1)}{1-\alpha} E_\alpha \left(-\frac{1}{1-\alpha}w^\alpha\right) ST\{E(t) - E(0)\} = ST[\alpha S(t)I(t) - \varepsilon_1 E(t)], \tag{7}$$

$$\frac{B(\alpha)\alpha\Gamma(\alpha+1)}{1-\alpha} E_\alpha \left(-\frac{1}{1-\alpha}w^\alpha\right) ST\{I(t) - I(0)\} = ST[rE(t) - \varepsilon_2 I(t)], \tag{8}$$

$$\frac{B(\alpha)\alpha\Gamma(\alpha+1)}{1-\alpha} E_\alpha \left(-\frac{1}{1-\alpha}w^\alpha\right) ST\{R(t) - R(0)\} = ST[\sigma_3 E(t) + \sigma_2 I(t) - d_1 R(t) + \sigma_1 Q(t)], \tag{9}$$

$$\frac{B(\alpha)\alpha\Gamma(\alpha+1)}{1-\alpha} E_\alpha \left(-\frac{1}{1-\alpha}w^\alpha\right) ST\{Q(t) - Q(0)\} = ST[\beta_1 E(t) + \beta_2 I(t) - \varepsilon_3 Q(t)]. \tag{10}$$

Rearranging and let $\Pi = \dfrac{1-\alpha}{B(\alpha)\alpha\Gamma(\alpha+1)E_\alpha\left(-\frac{1}{1-\alpha}w^\alpha\right)}$ then we get

$$ST(S(t)) = S(0) + \Pi \times ST[\Lambda - \alpha S(t)I(t) - d_1 S(t)]. \tag{11}$$

By using the inverse Sumudu transform of equation (11), we have

$$S(t) = S(0) + ST^{-1}\left[\Pi \times ST[\Lambda - \alpha S(t)I(t) - d_1 S(t)]\right]. \tag{12}$$

Therefore, the following is obtained.

$$S_{(n+1)}(t) = S_n(0) + ST^{-1}\left[\Pi \times ST[\Lambda - \alpha S_n(t)I_n(t) - d_1 S_n(t)]\right]. \tag{13}$$

The solution of equation (13), is

$$S(t) = \lim_{n\to\infty} S_n(t).$$

Similar for others.

$$E(t) = \lim_{n\to\infty} E_n(t), I(t) = \lim_{n\to\infty} I_n(t), \ R(t) = \lim_{n\to\infty} R_n(t), Q(t) = \lim_{n\to\infty} Q_n(t).$$

Theorem 4.1: Consider a Banach space $(X, |.|)$ and a self-map of X that satisfies

$$\|W_x - W_r\| \le \emptyset\|X - W_x\| + \emptyset\|x - r\|,$$

for all $x, r \in X$,and $0 \le \emptyset < 1$. Let W is Picard H-Stable. Suppose that in equation (13), we get

$$S_{(n+1)}(t) = S_n(0) + ST^{-1}\big[\Pi \times ST[\Lambda - \alpha S_n(t)I_n(t) - d_1 S_n(t)]\big].$$

Where Π is the fractional Lagrange multiplier, In the same manner for E,I,R,Q.

Theorem 4.2: Assume that K self-map is provided as

$$K\big[S_{(n+1)}(t)\big] = S_n(0) + ST^{-1}\big[\Pi \times ST[\Lambda - \alpha S_n(t)I_n(t) - d_1 S_n(t)]\big].$$

Proof: Taking the norm and applying the triangle inequality together yields

$$\|K[S_n(t)] - K[S_m(t)]\| \le \|S_n(t) - S_m(t)\| + ST^{-1}\big[\Pi \times ST\{\Lambda - \alpha\|(S_n(t)I_n(t) - S_m(t)I_m(t))\| - d_1\|(S_n(t) - S_m(t))\|\}\big]. \tag{14}$$

Similar for others.

Hence K satisfied all the conditions of Theorem (4.1), while

$$\emptyset = (0,0,0,0,0),$$

$$\emptyset$$

$$= \begin{cases} \|S_n(t) - S_m(t)\| \times \|-(S_n(t) + S_m(t))\| + \Lambda - \alpha\|(S_n(t)I_n(t) - S_m(t)I_m(t))\| \\ \quad -d_1\|(S_n(t) - S_m(t))\| \\ \times \|(E_n(t) - E_m(t))\| \times \|-(E_n(t) + E_m(t))\| + \alpha\|(S_n(t)I_n(t) - S_m(t)I_m(t))\| \\ \quad -\varepsilon_1\|(E_n(t) - E_m(t))\| \\ \times \|I_n(t) - I_m(t)\| \times \|-(I_n(t) + I_m(t))\| + r\|(E_n(t) - E_m(t))\| - \varepsilon_2\|(I_n(t) - I_m(t))\| \\ \times \|R_n(t) - R_m(t)\| \times \|-(R_n(t) + R_m(t))\| + \sigma_3\|(E_n(t) - E_m(t))\| + \sigma_2\|(I_n(t) - I_m(t))\| \\ \quad -d_1\|(R_n(t) - R_m(t))\| + \sigma_1\|(Q_n(t) - Q_m(t))\| \\ \times \|Q_n(t) - Q_m(t)\| \times \|-(Q_n(t) + Q_m(t))\| + \beta_1\|(E_n(t) - E_m(t))\| + \beta_2\|(I_n(t) - I_m(t))\| \\ \quad -\varepsilon_3\|Q_n(t) - Q_m(t)\|. \end{cases}$$

Consequently, it was demonstrated that K is Picard K-stable.

Theorem 4.3: Prove that equation (14), has a special and unique solution.

Proof: Let $Y = P^2\big((b,d) \times (0,T)\big)$ be the Hilbert space that is specified as

$$y: (b,d) \times (0,T) \to \mathbb{R}, \iint ghdgdh < \infty.$$

We consider

$$\theta(0,0,0,0,0), \theta = \begin{cases} \Lambda - \alpha S(t)I(t) - d_1 S(t), \\ \alpha S(t)I(t) - \varepsilon_1 E(t), \\ rE(t) - \varepsilon_2 I(t), \\ \sigma_3 E(t) + \sigma_2 I(t) - d_1 R(t) + \sigma_1 Q(t), \\ \beta_1 E(t) + \beta_2 I(t) - \varepsilon_3 Q(t). \end{cases}$$

We prove that the inner product of

$$T\big((S_{11} - S_{12}, E_{21} - E_{22}, I_{31} - I_{32}, R_{41} - R_{42}, Q_{51} - Q_{52}), (V_1, V_2, V_3, V_4, V_5)\big),$$

where the particular solutions to the system's equation are $(S_{11} - S_{12}, E_{21} - E_{22}, I_{31} - I_{32}, R_{41} - R_{42}, Q_{51} - Q_{52})$. Using the connection between the inner function and the norm, we can formulate the equation as

$$\big\{\Lambda - \alpha\big(S_{11}(t) - S_{12}(t)\big)\big(I_{31}(t) - I_{32}(t)\big) - d_1\big(S_{11}(t) - S_{12}(t)\big), V_1\big\} \leq \Lambda\|V_1\| - \alpha\|S_{11}(t) - S_{12}(t)\|\|I_{31}(t) - I_{32}(t)\|\|V_1\| - d_1\|S_{11}(t) - S_{12}(t)\|\|V_1\|,$$

$$\big\{\alpha\big(S_{11}(t) - S_{12}(t)\big)\big(I_{31}(t) - I_{32}(t)\big) - \varepsilon_1\big(E_{21}(t) - E_{22}(t)\big), V_2\big\} \leq \alpha\|S_{11}(t) - S_{12}(t)\|\|I_{31}(t) - I_{32}(t)\|\|V_2\| - \varepsilon_1\|E_{21}(t) - E_{22}(t)\|\|V_2\|,$$

$$\big\{r\big(E_{21}(t) - E_{22}(t)\big) - \varepsilon_2\big(I_{31}(t) - I_{32}(t)\big), V_3\big\} \leq r\|E_{21}(t) - E_{22}(t)\|\|V_3\| - \varepsilon_2\|I_{31}(t) - I_{32}(t)\|\|V_3\|,$$

$$\big\{\sigma_3\big(E_{21}(t) - E_{22}(t)\big) + \sigma_2\big(I_{31}(t) - I_{32}(t)\big) - d_1\big(R_{41}(t) - R_{42}(t)\big) + \sigma_1\big(Q_{51}(t) - Q_{52}(t)\big), V_4\big\} \leq \sigma_3\|E_{21}(t) - E_{22}(t)\|\|V_4\| + \sigma_2\|I_{31}(t) - I_{32}(t)\|\|V_4\| - d_1\|R_{41}(t) - R_{42}(t)\|\|V_4\| + \sigma_1\|Q_{51}(t) - Q_{52}(t)\|\|V_4\|,$$

$$\big\{\beta_1\big(E_{21}(t) - E_{22}(t)\big) + \beta_2\big(I_{31}(t) - I_{32}(t)\big) - \varepsilon_3\big(Q_{51}(t) - Q_{52}(t)\big), V_5\big\} \leq \beta_1\|E_{21}(t) - E_{22}(t)\|\|V_5\| + \beta_2\|I_{31}(t) - I_{32}(t)\|\|V_5\| - \varepsilon_3\|Q_{51}(t) - Q_{52}(t)\|\|V_5\|.$$

Due to a large number of e_1, e_2, e_3, e_4 and e_5, solutions approach an accurate response. We have the extremely small positive five parameters $\big(\chi_{e_1}, \chi_{e_2}, \chi_{e_3}, \chi_{e_4}$ and $\chi_{e_5}\big)$ after using the topology idea.

$$\|S - S_{11}\|, \|S - S_{12}\| \le \frac{\chi_{e_1}}{\varpi}, \|E - E_{21}\|, \|E - E_{22}\| \le \frac{\chi_{e_2}}{\varsigma}, \|I - I_{31}\|, \|I - I_{32}\| \le \frac{\chi_{e_3}}{\upsilon},$$

$$\|R - R_{41}\|, \|R - R_{42}\| \le \frac{\chi_{e_4}}{\kappa}, \text{ and } \|Q - Q_{51}\|, \|Q - Q_{52}\| \le \frac{\chi_{e_5}}{\varrho},$$

where

$$\varpi = 5(\Lambda - \alpha\|S_{11}(t) - S_{12}(t)\|\|I_{31}(t) - I_{32}(t)\| - d_1\|S_{11}(t) - S_{12}(t)\|)\|V_1\|,$$

$$\varsigma = 5(\alpha\|S_{11}(t) - S_{12}(t)\|\|I_{31}(t) - I_{32}(t)\| - \varepsilon_1\|E_{21}(t) - E_{22}(t)\|)\|V_2\|,$$

$$\upsilon = 5(r\|E_{21}(t) - E_{22}(t)\| - \varepsilon_2\|I_{31}(t) - I_{32}(t)\|)\|V_3\|,$$

$$\kappa = 5(\sigma_3\|E_{21}(t) - E_{22}(t)\| + \sigma_2\|I_{31}(t) - I_{32}(t)\| - d_1\|R_{41}(t) - R_{42}(t)\| + \sigma_1\|Q_{51}(t) - Q_{52}(t)\|)\|V_4\|,$$

$$\varrho = 5(\beta_1\|E_{21}(t) - E_{22}(t)\| + \beta_2\|I_{31}(t) - I_{32}(t)\| - \varepsilon_3\|Q_{51}(t) - Q_{52}(t)\|)\|V_5\|.$$

But, it is obvious that

$$(\Lambda - \alpha\|S_{11}(t) - S_{12}(t)\|\|I_{31}(t) - I_{32}(t)\| - d_1\|S_{11}(t) - S_{12}(t)\|) \ne 0,$$

$$(\alpha\|S_{11}(t) - S_{12}(t)\|\|I_{31}(t) - I_{32}(t)\| - \varepsilon_1\|E_{21}(t) - E_{22}(t)\|) \ne 0,$$

$$(r\|E_{21}(t) - E_{22}(t)\| - \varepsilon_2\|I_{31}(t) - I_{32}(t)\|) \ne 0,$$

$$(\sigma_3\|E_{21}(t) - E_{22}(t)\| + \sigma_2\|I_{31}(t) - I_{32}(t)\| - d_1\|R_{41}(t) - R_{42}(t)\| + \sigma_1\|Q_{51}(t) - Q_{52}(t)\|) \ne 0,$$

$$(\beta_1\|E_{21}(t) - E_{22}(t)\| + \beta_2\|I_{31}(t) - I_{32}(t)\| - \varepsilon_3\|Q_{51}(t) - Q_{52}(t)\|) \ne 0,$$

where $\|V_1\|, \|V_2\|, \|V_3\|, \|V_4\|, \|V_5\| \ne 0$.

So,

$$\|S_{11} - S_{12}\| = 0, \qquad \|E_{21} - E_{22}\| = 0, \qquad \|I_{31} - I_{32}\| = 0,$$

$$\|R_{41} - R_{42}\| = 0, \qquad \|Q_{51} - Q_{52}\| = 0.$$

Then

$$S_{11} = S_{12}, E_{21} = E_{22}, I_{31} = I_{32}, R_{41} = R_{42}, Q_{51} = Q_{52}.$$

So, the special solution is unique.

5. Chaos Control

In this section, we stabilize the system (5) using the linear feedback control method.

$$^{ABC}_{0}D^{\alpha}_{t}S = \Lambda - \alpha S(t)I(t) - d_1 S(t) + \xi(S - S_1),$$

$$^{ABC}_{0}D^{\alpha}_{t}E = \alpha S(t)I(t) - \varepsilon_1 E(t) + \xi(E - E_1),$$

$$^{ABC}_{0}D^{\alpha}_{t}I = rE(t) - \varepsilon_2 I(t) + \xi(I - I_1),$$

$$^{ABC}_{0}D^{\alpha}_{t}R = \sigma_3 E(t) + \sigma_2 I(t) - d_1 R(t) + \sigma_1 Q(t) + \xi(R - R_1),$$

$$^{ABC}_{0}D^{\alpha}_{t}Q = \beta_1 E(t) + \beta_2 I(t) - \varepsilon_3 Q(t) + \xi(Q - Q_1). \tag{15}$$

ξ are control variables, and the system equilibrium point is $E_\blacksquare$. For the system (15) the Jacobian matrix J at $E_\blacksquare$ can be derived as

$$J = \begin{bmatrix} -d_1 - \xi & 0 & -\dfrac{\Lambda}{d_1}\alpha & 0 & 0 \\ 0 & -\beta_1 - d_1 - r - \xi - \sigma_3 & \dfrac{\Lambda}{d_1}\alpha & 0 & 0 \\ 0 & r & -\beta_2 - d_1 - d_2 - \xi - \sigma_2 & 0 & 0 \\ 0 & \sigma_3 & \sigma_2 & -d_1 - \xi & \sigma_1 \\ 0 & \beta_1 & \beta_2 & 0 & -d_1 - d_2 - \xi - \sigma_1 \end{bmatrix},$$

The Jacobian matrix J, its characteristic equation is

$$f(\lambda) = \begin{bmatrix} \lambda + d_1 + \xi & 0 & -\dfrac{\Lambda}{d_1}\alpha & 0 & 0 \\ 0 & \lambda + \beta_1 + d_1 + r + \xi + \sigma_3 & \dfrac{\Lambda}{d_1}\alpha & 0 & 0 \\ 0 & r & \lambda + \beta_2 + d_1 + d_2 + \xi + \sigma_2 & 0 & 0 \\ 0 & \sigma_3 & \sigma_2 & \lambda + d_1 + \rho & \sigma_1 \\ 0 & \beta_1 & \beta_2 & 0 & \lambda + d_1 + d_2 + \xi + \sigma_1 \end{bmatrix},$$

characteristic polynomial

$$C(\lambda) = \lambda^5 + B_1\lambda^4 + B_2\lambda^3 + B_3\lambda^2 + B_4\lambda^1 + B_5,$$

$$C(\lambda) = \lambda^5 - 5.1609\lambda^4 - 10.2432\lambda^3 - 10.1634\lambda^2 - 5.0412\lambda^1 - 1.0399. \tag{16}$$

Where

$$\lambda_1 = -3.0 \times 10^{-5}, \quad \lambda_2 = -0.3197, \ \lambda_3 = -6.97 \times 10^{-3}, \lambda_4 = -3.0 \times 10^{-5},$$

$$\lambda_5 = -9.70 \times 10^{-5}.$$

Equations (16) exhibit asymptotic stability at equilibrium points $E_\blacksquare$ because each eigenvalue is either a complex number with a negative real component or a negative real number.

6. New Numerical Scheme

In the context of the Coronavirus outbreak [29], we define the Atangana-Toufik suggested technique described in [15] for the fractional derivative SEIQR model with equations (5).

Let $\Psi = \dfrac{(1-\alpha)}{ABC(\alpha)}$, $\Phi = \dfrac{\alpha}{\Gamma(\alpha) \times ABC(\alpha)}$. From equations (5)

$$S(t) - S(0) = \Psi\{\Lambda - \alpha S(t)I(t) - d_1 S(t)\} + \Phi \int_0^t \{\Lambda - \alpha S(\tau)I(\tau) - d_1 S(\tau)\}(t-\tau)^{\alpha-1}d\tau,$$

$$E(t) - E(0) = \Psi\{\alpha S(t)I(t) - \varepsilon_1 E(t)\} + \Phi \int_0^t \{\alpha S(\tau)I(\tau) - \varepsilon_1 E(\tau)\}(t-\tau)^{\alpha-1}d\tau,$$

$$I(t) - I(0) = \Psi\{rE(t) - \varepsilon_2 I(t)\} + \Phi \int_0^t \{rE(\tau) - \varepsilon_2 I(\tau)\}(t-\tau)^{\alpha-1}d\tau,$$

$R(t) - R(0) = \Psi\{\sigma_3 E(t) + \sigma_2 I(t) - d_1 R(t) + \sigma_1 Q(t)\} + \Phi \int_0^t \{\sigma_3 E(\tau) + \sigma_2 I(\tau) - d_1 R(\tau) + \sigma_1 Q(\tau)\}(t - \tau)^{\alpha-1} d\tau,$

$Q(t) - Q(0) = \Psi\{\beta_1 E(t) + \beta_2 I(t) - \varepsilon_3 Q(t)\} + \Phi \int_0^t \{\beta_1 E(\tau) + \beta_2 I(\tau) - \varepsilon_3 Q(\tau)\}(t - \tau)^{\alpha-1} d\tau.$ (17)

At $t_{n+1}, n = 0,1,2,3, ...,$ we have

$S(t_{n+1}) - S(0) = \Psi\{\Lambda - \alpha S(t_n)I(t_n) - d_1 S(t_n)\} + \Phi \int_0^{t_{n+1}} \{\Lambda - \alpha S(\tau)I(\tau) - d_1 S(\tau)\}(t_{n+1} - \tau)^{\alpha-1} d\tau,$

$E(t_{n+1}) - E(0) = \Psi\{\alpha S(t_n)I(t_n) - \varepsilon_1 E(t_n)\} + \Phi \int_0^{t_{n+1}} \{\alpha S(\tau)I(\tau) - \varepsilon_1 E(\tau)\}(t_{n+1} - \tau)^{\alpha-1} d\tau,$

$I(t_{n+1}) - I(0) = \Psi\{rE(t_n) - \varepsilon_2 I(t_n)\} + \Phi \int_0^{t_{n+1}} \{rE(\tau) - \varepsilon_2 I(\tau)\}(t_{n+1} - \tau)^{\alpha-1} d\tau,$

$R(t_{n+1}) - R(0) = \Psi\{\sigma_3 E(t_n) + \sigma_2 I(t_n) - d_1 R(t_n) + \sigma_1 Q(t_n)\} + \Phi \int_0^{t_{n+1}} \{\sigma_3 E(\tau) + \sigma_2 I(\tau) - d_1 R(\tau) + \sigma_1 Q(\tau)\}(t_{n+1} - \tau)^{\alpha-1} d\tau,$

$Q(t_{n+1}) - Q(0) = \Psi\{\beta_1 E(t_n) + \beta_2 I(t_n) - \varepsilon_3 Q(t_n)\} + \Phi \int_0^{t_{n+1}} \{\beta_1 E(\tau) + \beta_2 I(\tau) - \varepsilon_3 Q(\tau)\}(t_{n+1} - \tau)^{\alpha-1} d\tau.$ (18)

Also, we have

$S(t_{n+1}) - S(0) = \Psi\{\Lambda - \alpha S(t_n)I(t_n) - d_1 S(t_n)\} + \Phi \sum_{j=0}^n \int_{t_j}^{t_{j+1}} \{\Lambda - \alpha S(\tau)I(\tau) - d_1 S(\tau)\}(t_{n+1} - \tau)^{\alpha-1} d\tau,$

$E(t_{n+1}) - E(0) = \Psi\{\alpha S(t_n)I(t_n) - \varepsilon_1 E(t_n)\} + \Phi \sum_{j=0}^n \int_{t_j}^{t_{j+1}} \{\alpha S(\tau)I(\tau) - \varepsilon_1 E(\tau)\}(t_{n+1} - \tau)^{\alpha-1} d\tau,$

$I(t_{n+1}) - I(0) = \Psi\{rE(t_n) - \varepsilon_2 I(t_n)\} + \Phi \sum_{j=0}^n \int_{t_j}^{t_{j+1}} \{rE(\tau) - \varepsilon_2 I(\tau)\}(t_{n+1} - \tau)^{\alpha-1} d\tau,$

$$R(t_{n+1}) - R(0) = \Psi\{\sigma_3 E(t_n) + \sigma_2 I(t_n) - d_1 R(t_n) + \sigma_1 Q(t_n)\} + \Phi \sum_{j=0}^{n} \int_{t_j}^{t_{j+1}} \{\sigma_3 E(\tau) +$$

$$\sigma_2 I(\tau) - d_1 R(\tau) + \sigma_1 Q(\tau)\}(t_{n+1} - \tau)^{\alpha-1} d\tau,$$

$$Q(t_{n+1}) - Q(0) = \Psi\{\beta_1 E(t_n) + \beta_2 I(t_n) - \varepsilon_3 Q(t_n)\} + \Phi \sum_{j=0}^{n} \int_{t_j}^{t_{j+1}} \{\beta_1 E(\tau) + \beta_2 I(\tau) -$$

$$\varepsilon_3 Q(\tau)\}(t_{n+1} - \tau)^{\alpha-1} d\tau. \tag{19}$$

Now, we have

$$S_{n+1} = S_0 + \Psi\{\Lambda - \alpha S(t_n)I(t_n) - d_1 S(t_n)\} + \Phi \sum_{j=0}^{n} \left(\frac{\{\Lambda - \alpha S_j I_j - d_1 S_j\}}{h} \int_{t_j}^{t_{j+1}} (\tau - t_{j-1})(t_{n+1} -$$

$$\tau)^{\alpha-1} d\tau - \frac{\{\Lambda - \alpha S_{j-1} I_{j-1} - d_1 S_{j-1}\}}{h} \int_{t_j}^{t_{j+1}} (\tau - t_j)(t_{n+1} - \tau)^{\alpha-1} d\tau \right),$$

$$E_{n+1} = E_0 + \Psi\{\alpha S(t_n)I(t_n) - \varepsilon_1 E(t_n)\} + \Phi \sum_{j=0}^{n} \left(\frac{\{\alpha S_j I_j - \varepsilon_1 E_j\}}{h} \int_{t_j}^{t_{j+1}} (\tau - t_{j-1})(t_{n+1} -$$

$$\tau)^{\alpha-1} d\tau - \frac{\{\alpha S_{j-1} I_{j-1} - \varepsilon_1 E_{j-1}\}}{h} \int_{t_j}^{t_{j+1}} (\tau - t_j)(t_{n+1} - \tau)^{\alpha-1} d\tau \right),$$

$$I_{n+1} = I_0 + \Psi\{rE(t_n) - \varepsilon_2 I(t_n)\} + \Phi \sum_{j=0}^{n} \left(\frac{\{rE_j - \varepsilon_2 I_j\}}{h} \int_{t_j}^{t_{j+1}} (\tau - t_{j-1})(t_{n+1} - \tau)^{\alpha-1} d\tau -$$

$$\frac{\{rE_{j-1} - \varepsilon_2 I_{j-1}\}}{h} \int_{t_j}^{t_{j+1}} (\tau - t_j)(t_{n+1} - \tau)^{\alpha-1} d\tau \right),$$

$$R_{n+1} =$$

$$R_0 + \Psi\{\sigma_3 E(t_n) + \sigma_2 I(t_n) - d_1 R(t_n) + \sigma_1 Q(t_n)\} + \Phi \sum_{j=0}^{n} \left(\frac{\{\sigma_3 E_j + \sigma_2 I_j - d_1 R_j + \sigma_1 Q_j\}}{h} \int_{t_j}^{t_{j+1}} (\tau -$$

$$t_{j-1})(t_{n+1} - \tau)^{\alpha-1} d\tau - \frac{\{\sigma_3 E_{j-1} + \sigma_2 I_{j-1} - d_1 R_{j-1} + \sigma_1 Q_{j-1}\}}{h} \int_{t_j}^{t_{j+1}} (\tau - t_j)(t_{n+1} - \tau)^{\alpha-1} d\tau \right),$$

$$Q_{n+1} = Q_0 + \Psi\{\beta_1 E(t_n) + \beta_2 I(t_n) - \varepsilon_3 Q(t_n)\} + \Phi \sum_{j=0}^{n} \left(\frac{\{\beta_1 E_j + \beta_2 I_j - \varepsilon_3 Q_j\}}{h} \int_{t_j}^{t_{j+1}} (\tau -$$

$$t_{j-1})(t_{n+1} - \tau)^{\alpha-1} d\tau - \frac{\{\beta_1 E_{j-1} + \beta_2 I_{j-1} - \varepsilon_3 Q_{j-1}\}}{h} \int_{t_j}^{t_{j+1}} (\tau - t_j)(t_{n+1} - \tau)^{\alpha-1} d\tau \right).$$

As a result, integrating the above equations

$$\Omega = \{(n + 1 - j)^{\alpha}(n - j + 2 + \alpha) - (n - j)^{\alpha}(n - j + 2 + 2\alpha)\},$$

$$\Theta = \{(n+1-j)^{\alpha+1} - (n-j)^\alpha(n-j+1+\alpha)\},$$

$$S_{n+1} =$$
$$S_0 + \Psi\{\Lambda - \alpha S(t_n)I(t_n) - d_1 S(t_n)\} + \Phi \sum_{j=0}^{n} \left(\frac{\{\Lambda - \alpha S_j I_j - d_1 S_j\}}{h} \Omega - \frac{\{\Lambda - \alpha S_{j-1} I_{j-1} - d_1 S_{j-1}\}}{h} \Theta \right),$$

$$E_{n+1} = E_0 + \Psi\{\alpha S(t_n)I(t_n) - \varepsilon_1 E(t_n)\} + \Phi \sum_{j=0}^{n} \left(\frac{\{\alpha S_j I_j - \varepsilon_1 E_j\}}{h} \Omega - \frac{\{\alpha S_{j-1} I_{j-1} - \varepsilon_1 E_{j-1}\}}{h} \Theta \right),$$

$$I_{n+1} = I_0 + \Psi\{rE(t_n) - \varepsilon_2 I(t_n)\} + \Phi \sum_{j=0}^{n} \left(\frac{\{rE_j - \varepsilon_2 I_j\}}{h} \Omega - \frac{\{rE_{j-1} - \varepsilon_2 I_{j-1}\}}{h} \Theta \right),$$

$$R_{n+1} = R_0 + \Psi\{\sigma_3 E(t_n) + \sigma_2 I(t_n) - d_1 R(t_n) + \sigma_1 Q(t_n)\} + \Phi \sum_{j=0}^{n} \left(\frac{\{\sigma_3 E_j + \sigma_2 I_j - d_1 R_j + \sigma_1 Q_j\}}{h} \Omega - \right.$$
$$\left. \frac{\{\sigma_3 E_{j-1} + \sigma_2 I_{j-1} - d_1 R_{j-1} + \sigma_1 Q_{j-1}\}}{h} \Theta \right),$$

$$Q_{n+1} =$$
$$Q_0 + \Psi\{\beta_1 E(t_n) + \beta_2 I(t_n) - \varepsilon_3 Q(t_n)\} +$$
$$\Phi \sum_{j=0}^{n} \left(\frac{\{\beta_1 E_j + \beta_2 I_j - \varepsilon_3 Q_j\}}{h} \Omega - \frac{\{\beta_1 E_{j-1} + \beta_2 I_{j-1} - \varepsilon_3 Q_{j-1}\}}{h} \Theta \right).$$

7. Results and Discussion

The COVID-19 SEIRQ fractional order model can be utilized for analysis and simulation in order to examine the dynamic behavior of disease transmission in society. Specifically, we applied the Atangana Toufik scheme and ABC with Mittag-Leffler law to the Covid-19 SEIRQ model, using initial conditions S(0)= 34,218,169, E(0)=5.0×10^3, I(0)=157, R(0)=99, Q(0)=1720. In [29] provides further information on the parameter values are $\beta_1 = 0.02$, $\beta_2 = 0.005$, $\sigma_1 = 0.001$, $\sigma_2 = 0.002$, $\sigma_3 = 0.002$, r=0.01, $d_1 = 3.0 \times 10^{-5}$, $d_2 = 3.5 \times 10^{-7}$. In this study, a novel numerical technique for the recently established fractional differentiation has been proposed. By using the ABC fractional derivative, distinct fractional values are obtained for the numerical result based on the steady-state point. Various numerical techniques are observed to investigate the impact of the given time parameter on the fractional order model mechanics. The

model's dynamics changed and this was revealed through simulations. The memory effects of nonlinear systems are also observed with the help of fractional value results. It provides a new approach to the targeted value to manage the disease without establishing additional criteria. Figures 4-8 provide graphs that tell about solutions against different fractional order α. The steady-state equilibrium points are bounded by the sub-compartment of the system. In Figure 4 the susceptible population S(t) over time, showing how varying fractional orders α affect the model. When decrease values of α typically introduce memory effects and non-local interactions, implying that past states of the system impact current susceptibility levels. This is crucial in understanding how a susceptible individual's risk of infection fluctuates over time with fractional dynamics. The fractional order variation in fig 5 highlights the latency dynamics within this group, which can influence the timing and size of infection waves as exposed individuals transition to infection states at different rates based on the memory parameter α. The fractional order impact in fig 6 shows potential delays or accelerations in infection progression, which are significant for anticipating peak infection rates and managing healthcare resources. Fractional-order variations in fig 7 illustrate how recovery dynamics evolve, potentially impacting herd immunity thresholds and the population's resilience to future outbreaks. In fig 8 evaluates the effectiveness of quarantine measures, where different values of α reflect varying degrees of adherence or effectiveness in isolating infected individuals. The current non-integer-order types have less advantage as compared to these operators. This model was developed using data acquired from print or media sources regarding the causative agent and virus transmission model.
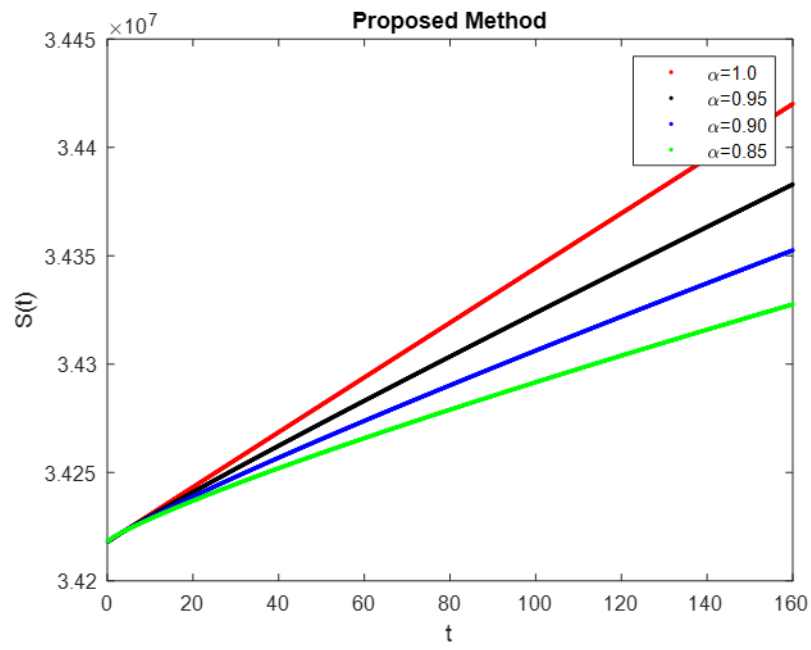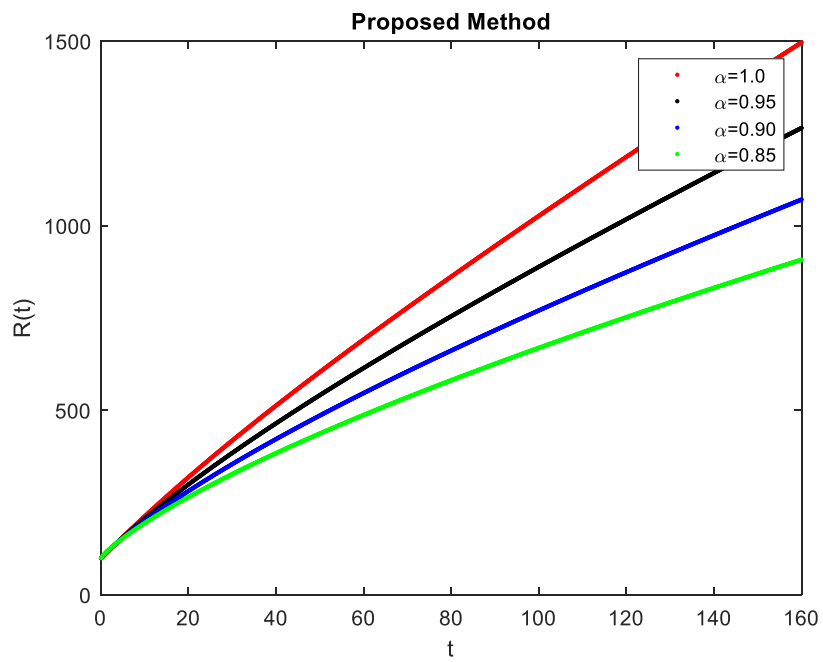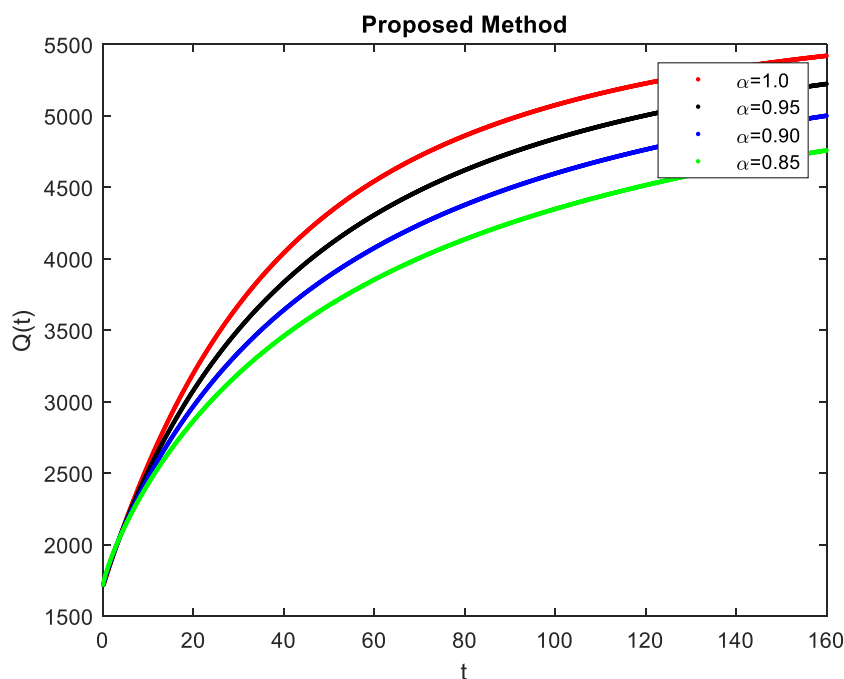
Figure 4: Simulation of S(t) with fractional order
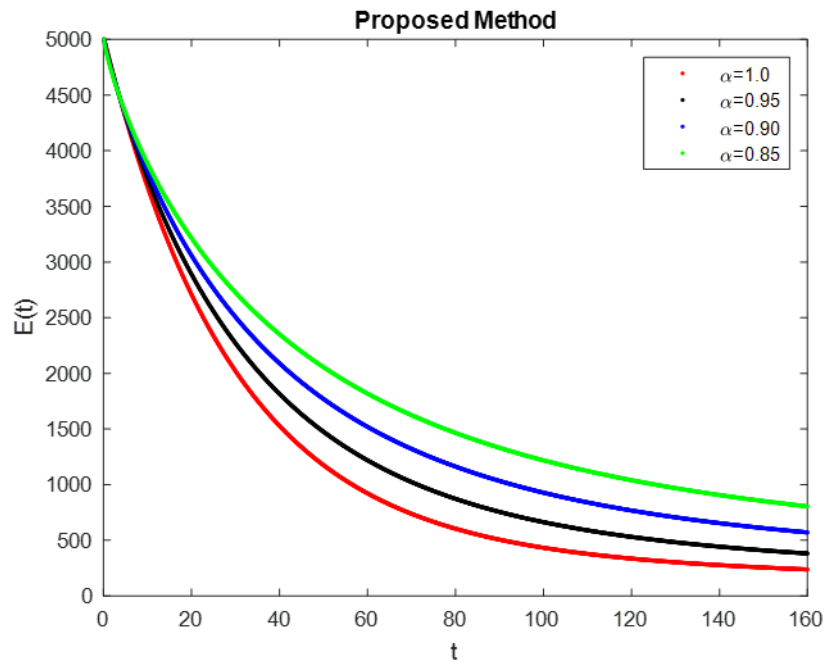
Figure 5: Simulation of E(t) with fractional order
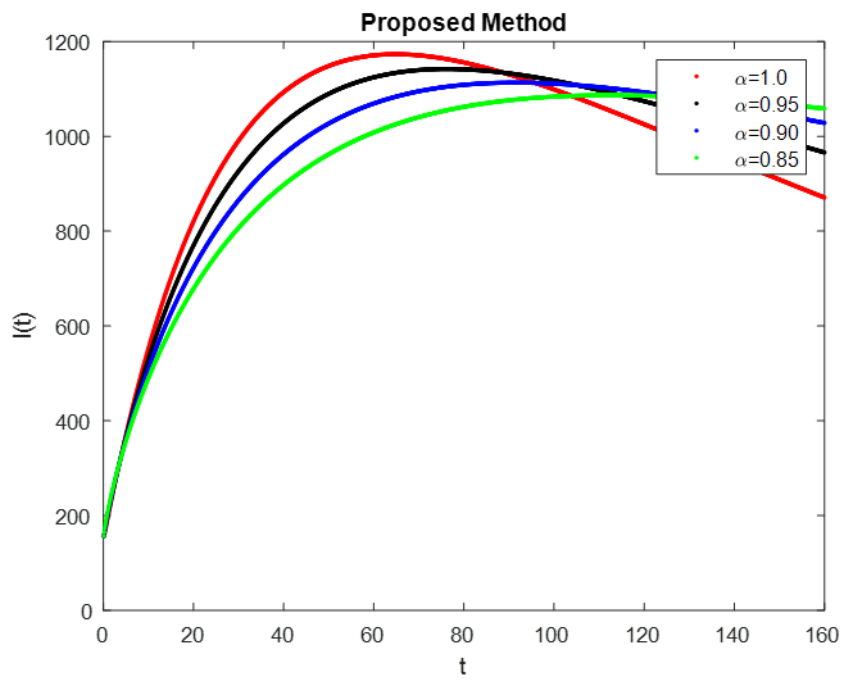
Figure 6: Simulation of I(t) with fractional order

Figure 7: Simulation of R(t) with fractional order

Figure 8: Simulation of Q(t) with fractional order

8. Conclusion

In this article, we used the Mittag-Leffler kernel and the ABC fractional derivative to study the COVID-19 fractional model. The iterative approach and fixed-point theory were utilized to determine the existence solution of the model. Utilizing the proposed model, we were able to attain highly significant results. In the context of fractional calculus, non-singular and non-local kernels were employed to derive non-linear fractional differential equations from the derivative. The sick individuals received a variety of therapy approaches, such as medications, vitamins, and tones, which were also supplied to the uninfected individuals. According to the memory effect, the dynamics of the epidemiological system are shaped by the peaks and magnitudes of infection, which increase with the epidemic system's "memory" of previous states.

The utilization of the Mittag-Leffler kernel in conjunction with the ABC fractional derivative significantly augments the modeling potential for the investigation of COVID-19 dynamics by providing enhanced flexibility, precision, and resilience in simulations. These methodologies empower researchers to gain a more profound comprehension and forecasting capability regarding the intricate behaviors linked to epidemic occurrences. Through the analysis of this

model, we may create more accurate plans to reduce the impact of epidemics, which will ultimately result in the saving of lives and better community recovery.

References:

1. W. Gao, P. Veeresha, D.G. Prakasha, HM. Baskonus and G. Yel. New approach for the model describing the deathly disease in pregnant women using Mittag-Leffler function. *Chaos, Solitons and Fractals* (2020), *134,* 109696.
2. M. Goyal, H.M. Baskonus and A. Prakash. An efficient technique for a time fractional model of lassa hemorrhagic fever spreading in pregnant women. *The European Physical Journal Plus* (2019) *134*, 482.
3. D. Kumar, J. Singh, M. Al Qurashi and D. Baleanu. A new fractional SIRS-SI malaria disease model with application of vaccines, antimalarial drugs, and spraying. *Advances in Difference Equations* 2019, *2019* (1-19).
4. S. Jamil, P.A. Naik, M. Farman, M.U. Saleem, A.H. Ganie. Stability and complex dynamical analysis of COVID-19 epidemic model with non-singular kernel of Mittag-Leffler law. *Journal of Applied Mathematics and Computing,* 2024, (1-36).
5. Ahmad. A Review of COVID-19 (Coronavirus Disease-2019) Diagnosis, Treatments and Prevention. *Authorea Preprints* 2022, *4(2),* 116-125.
6. R.N.Thompson, T.D. Hollingsworth, V. Isham, D. Arribas-Bel, B. Ashby, T. Britton, P. Challenor, L.H. Chappell, H. Clapham, N.J. Cunniffe, A.P. Dawid. Key questions for modelling COVID-19 exit strategies. *Proceedings of the Royal Society B* 2020, *287*, 20201405.

7. M. Caputo, M. Fabrizio. A new definition of fractional derivative without singular kernel. *Prog. Fract. Differ. Appl.* (2015) *2,* 73–85.
8. A. Atangana, D. Baleanu. New fractional derivatives with nonlocal and non-singular kernel Theory and application to heat transfer model, *arXiv preprint arXiv:1602.03408* (2016).
9. M. Farman, M.U. Saleem, M.F. Tabassum, A. Ahmad, M.O Ahmad. A Linear Control of Composite model for Glucose Insulin Glucagon, *AinShamas Engineering Journal* (2019),*10,* 867-872.
10. M. Farman, M.U. Saleem, A. Ahmad, S. Imtiaz, M.F. Tabassm, S. Akram, M.O. Ahmad. A Control of Glucose Level in Insulin Therapies for the Development of Artificial Pancreas by Atangana-Baleanu Fractional Derivative, *Alexandria Engineering Journal* (2020), *59, 2639-2648.
11. M. Farman, A. Akgül, D. Baleanu, S. Imtiaz, A. Ahmad. Analysis of Fractional Order Chaotic Financial Model with Minimum Interest Rate Impact, *Fractal and Fractional* (2020) *4,* 43.
12. Y. Zi and Y. Wang. (2019). Positive solutions for Caputo fractional differential system with coupled boundary conditions. *Advances in Difference Equations* (2019), (2019) 1-12.
13. M. Toufik, A. Atangana. New numerical approximation of fractional derivative with non-local and non-singular kernel: Application to chaotic models. *Eur. Phys. J. Plus* (2017) *132,*444.
14. Z. Liu, Y. Ding, C. Liu and C. Zhao. Existence and uniqueness of solutions for singular fractional differential equation boundary value problem with p-Laplacian. *Advances in Difference Equations* (2020), *2020,* 83.
15. Y. Wang and L. Liu. Uniqueness and existence of positive solutions for the fractional integro-differential equation. *Boundary Value Problems* (2017), 2017, 1-17.

16. H. Azhar, B. Dumitru, Y. Saman. On a nonlinear fractional-order model of novel coronavirus (NCOV-2019) under AB-fractional derivative. *Journal of Mathematical Extension* (2021), *15.*

17. M.A Khan, A. Atangana. Modeling the dynamics of novel coronavirus (2019- NCOV) with fractional derivative. *Alexandria Eng J* (2020), *59(4),* 2379-2389.

18. A. Atangana, E. Bonyah, A.A Elsadany. A fractional order optimal 4D chaotic financial model with Mittag-Leffler law, *Chinese Journal of Physics,* (2020). *65**,* 38-53.

19. J.T Wu, K. Leung, G.M. Leung. Nowcasting and forecasting the potential domestic and international spread of the 2019-nCoV outbreak originating in Wuhan, China: a modelling study. *The Lancet* (2020) *395,* 689–697.

20. B. Tang, N. Bragazzi, Q. Li, S. Tang, Y. Xiao, W. Jianhong. An updated estimation of the risk of transmission of the novel coronavirus (2019-nCov). *Infect. Dis. Model* (2020),*5,* 248–255.

21. E.K. Akgül. Solutions of the linear and nonlinear differential equations within the generalized fractional derivatives, *Chaos: An Interdisciplinary Journal of Nonlinear Science* (2019) *29 (2),* 023108.

22. A. Atangana, A. Akgül. Can transfer function and Bode diagram be obtained from Sumudu transform, *Alexandria Engineering Journal* (2020), *59*, 1971-1984.

23. M.S. Hashemi, D. Baleanu. Lie symmetry analysis of fractional differential equations, *CRC Press* (2020).

24. M.S. Hashemi, M. Inc, A. Yusuf. On three-dimensional variable order time fractional chaotic system with nonsingular kernel, *Chaos, Solitons and Fractals* (2020), *133,* 109628.

25. M.S. Hashemi, A. Akgül. Solitary wave solutions of time-space nonlinear fractional Schrodinger's equation: Two analytical approaches, *JOURNAL OF COMPUTATIONAL AND APPLIED MATHEMATICS* (2018), *339,* 147-160.

26. M.S. Hashemi. A novel approach to find exact solutions of fractional evolution equations with non-singular kernel derivative*, Chaos, Solitons & Fractals* (2021)**,** *152*, 111367.

27. H. Li and Y. Wu. Dynamics of SCIR Modeling for COVID-19 with Immigration. *Complexity* (2022), *2022,* 9182830.

28. P. Shao and S. Shateyi. Stability analysis of SEIRS epidemic model with nonlinear incidence rate function. *Mathematics* (2021), *21*, 2644.

29. H. Youssef, N. Alghamdi, M.A. Ezzat, A.A. El-Bary, A.M. Shawky. A New Dynamical Modelling of the Epidemic Diseases to Assessing the Rates of Spread of COVID-19 in Saudi Arabia: SEIRQ Model*, Scientific Reports*, Nature Research, DOI: 10.21203/rs.3.rs-77792/v1, (2020).